Quantifying biological carbon export for the northwest North Atlantic continental shelves

Katja Fennel[1] and John Wilkin[2]

Received 29 June 2009; revised 18 August 2009; accepted 27 August 2009; published 19 September 2009.

[1] It has been suggested that continental shelf systems contribute disproportionately to the oceanic uptake of atmospheric CO_2, but the magnitude of this flux and the relative contributions of different underlying mechanisms are poorly quantified. A biological continental shelf pump mechanism has been implied; however, the magnitude of this export depends on advective transport of carbon-rich water off the shelf, a process that is difficult to observe directly. Here we use a physical-biogeochemical model for the northeastern North American continental margin to estimate the uptake of atmospheric CO_2, the fraction of this uptake that results from biological processes, and the transport of organic carbon off the shelf. Our results suggest that there is no systematic difference in the area-normalized CO_2 uptake between the shelf regions and the adjacent deep ocean. The advective transport of carbon-rich water off the shelf is insufficient to drive a Continental Shelf Pump in this region. **Citation:** Fennel, K., and J. Wilkin (2009), Quantifying biological carbon export for the northwest North Atlantic continental shelves, *Geophys. Res. Lett.*, *36*, L18605, doi:10.1029/2009GL039818.

1. Introduction

[2] The ocean has taken up ~50% of anthropogenic CO_2 emissions and thus slowed the accumulation of anthropogenic CO_2 in the atmosphere, but the strength of the ocean sink is likely to diminish in the future [*Sabine et al.*, 2004]. Many aspects of oceanic CO_2 uptake, including its magnitude, where it occurs, and by which mechanisms, are poorly understood and limit our ability to predict the strength of the ocean sink in the future. It has been suggested that continental shelf systems contribute disproportionately to the oceanic uptake of CO_2, for example, large uptake fluxes have been estimated based on observations for the East China Sea [*Tsunogai et al.*, 1999], the Chukchi Sea [*Bates*, 2006], the North Sea [*Thomas et al.*, 2004] and the Middle Atlantic Bight (MAB) [*DeGrandpre et al.*, 2002]. Two recent compilations of observational estimates document that variability in coastal CO_2 fluxes is large, but suggest a general pattern of mid- and high-latitude systems acting as sinks of atmospheric CO_2, while subtropical and tropical regions act as sources [*Cai et al.*, 2006; *Borges et al.*, 2005]. *Borges et al.* [2005] and *Cai et al.* [2006] arrive at different global estimates of continental shelf uptake (0.45 Pg C yr^{-1} versus 0.22 Pg C yr^{-1}, respectively), illustrating the large uncertainty in extrapolations from local to global estimates.

[3] Different mechanisms have been suggested to drive the enhanced CO_2 uptake in shelf systems and are collectively referred to as the continental shelf pump (CSP). The large uptake estimates for the Chukchi Sea and the North Sea were attributed to a biological CSP mechanism by which production of organic matter results in CO_2 undersaturation in the surface, driving uptake of CO_2, and subsequent sinking and export of organic matter off the shelf [*Bates*, 2006; *Thomas et al.*, 2004]. This allows for the biologically-fixed carbon to be transported to the deep ocean and protected from re-exposure at the surface with subsequent winter mixing. The mechanism thus depends on the horizontal transport (advection and mixing) of organic matter, which is hard to observe or quantify directly. Here we use a coupled physical-biogeochemical model to estimate the uptake of atmospheric CO_2, quantify the biologically driven fraction of this uptake, and estimate the horizontal export of organic matter off the shelf for the northeastern North American continental margin.

2. Model Description

[4] Our model is a high-resolution implementation of the Regional Ocean Modeling System (ROMS, http://www.myroms.org) [*Haidvogel et al.*, 2008] for the continental shelf area of the North American east coast and adjacent deep ocean. The model has a horizontal grid resolution of approximately 10 km, and uses 30 vertical layers in a terrain-following *s*-coordinate system. We specified the model's open boundary temperatures, salinities and transports from the data-assimilative Hybrid Coordinate Ocean Model (HyCOM, http://hycom.org) of *Chassignet et al.* [2007] and augmented the HyCOM open boundary transports with barotropic tides from the global analysis of *Egbert and Erofeeva* [2002]. HyCOM temperatures and salinities were biased compared to the Hydrobase climatology [*Lozier et al.*, 1995] so this bias was removed by adjusting the HyCOM temporal mean to match Hydrobase. These modified HyCOM values determine the ROMS open boundary conditions. We forced the model with air temperature, pressure, humidity and winds from the daily NCEP reanalysis [*Kalnay et al.*, 1996] using bulk formulae [*Fairall et al.*, 2003].

[5] The biogeochemical model consists of the nitrogen cycle model with parameterized sediment denitrification described by *Fennel et al.* [2006] and a model of carbonate chemistry based on the standard set by the Ocean Carbon-Cycle Model Intercomparison Project Phase 2 (J. C. Orr et al., Abiotic-HOWTO, Internal OCMIP Report, 25 pp., LSCE/CEA Saclay, Gif-sur-Yvette, France, 1999; available

[1]Department of Oceanography, Dalhousie University, Halifax, Nova Scotia, Canada.
[2]Institute of Marine and Coastal Sciences, Rutgers, State University of New Jersey, New Brunswick, New Jersey, USA.

0094-8276/09/2009GL039818$05.00

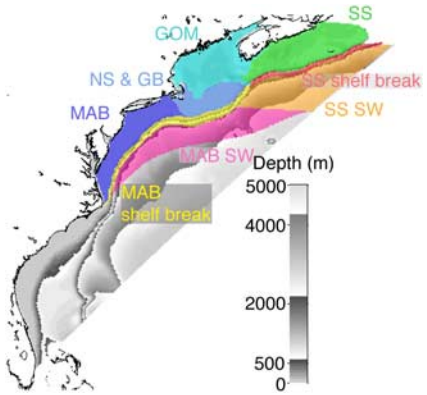

Figure 1. Model bathymetry (grayscale) overlain by subregions (color) that we used for spatial integration. NS&GB represents the tidally mixed area, which includes Nantucket Shoals and Georges Bank. GOM refers to the Gulf of Maine. SS represents the Scotian Shelf. We combined the narrow regions MAB shelf break and SS shelf break with the adjacent slope water regions for spatial integration and refer to the combined regions as MAB SB + SW and SS SB + SW.

at http://www.ipsl.jussieu.fr/OCMIP/phase2/simulations/Abiotic/HOWTO-Abiotic.html). Knowledge of any two of the six variables of the carbonate system (total dissolved inorganic carbon [DIC], pCO_2, carbonate ion concentration, bicarbonate ion concentration, pH and alkalinity) determines the remaining four, but only DIC and alkalinity behave conservatively with respect to mixing and temperature and pressure changes [*Zeebe and Wolf-Gladrow*, 2001]. DIC and alkalinity are thus included as active tracers (i.e., they are advected and diffused by the physical model), while pCO_2, the carbon variable relevant for air-sea gas exchange of CO_2, is calculated in the surface model layer only. Local changes in DIC occur due to primary production, respiratory processes and gas exchange at the air-sea interface. We parameterized gas exchange following *Wanninkhof* [1992] and initialized DIC and alkalinity using the *T*- and *S*-dependent relationships derived by *Lee et al.* [2000] and *Millero et al.* [1998], respectively. Nitrogen and organic carbon inputs from rivers were prescribed to match the annual mean values from a watershed analysis [*Dumont et al.*, 2005], but were modulated by monthly freshwater fluxes observed at US Geological Survey gauging stations. Riverine alkalinity values were determined using *Millero et al.*'s [1998] relationship for $S = 0$; DIC was assumed to be in equilibrium with atmospheric values of CO_2 in the river sources. We ran the model for the years 2004 and 2005 after a six-month spin-up period that started in June 2003. This simulation is identical to the implementation by *Fennel et al.* [2008] and we refer to it below as the baseline simulation.

[6] We then ran one-year simulations, initialized with fields for January 1, 2004 and 2005, with all biological sources and sinks of DIC and alkalinity disabled (which we refer to as no-bio simulations) and estimated the fraction of air-sea CO_2 flux directly attributable to biological processes from the difference between the baseline flux and the no-bio flux. In order to quantify the horizontal export of organic carbon off the shelf, we calculated the horizontal divergence of organic carbon. Specifically, we calculate integrals of the vertically integrated divergence of organic carbon ($-\int\int \nabla \cdot (\boldsymbol{u}C)\, dz\, dt$ where $\boldsymbol{u}$ is the three-dimensional velocity, C is the concentration of organic carbon, z is depth, and t is time) for each model grid cell. The vertical integral is over the whole water column; the temporal integral is over the calendar years 2004 and 2005. By further integrating these divergences spatially we infer the net export of organic carbon for the shelf regions shown in Figure 1.

3. Results

[7] Here we focus on the simulated air-sea CO_2 fluxes, the relative contribution of biological processes to this flux and the off-shelf transport of organic carbon. It has been shown by *Fennel et al.* [2008] that simulated surface pCO_2 agrees with available observations in the MAB and that the biological model component predicts primary production and spatial and temporal patterns in surface chlorophyll realistically.

[8] Four representative snapshots (Figure 2) of the modeled pCO_2 difference between the atmosphere and ocean surface illustrate the magnitude and direction of the air-sea flux of CO_2. The air-sea fluxes are driven by two major processes: changes in the solubility of CO_2 due to changes in ocean temperature, and production and respiration of organic matter, which decreases/increases the concentration of dissolved inorganic carbon (DIC). Changes in salinity and alkalinity also affect the seawater pCO_2 and thus the air-sea flux, but these effects are of second-order importance. In February, the model predicts uptake of atmospheric CO_2 across the whole domain, with the largest fluxes in the

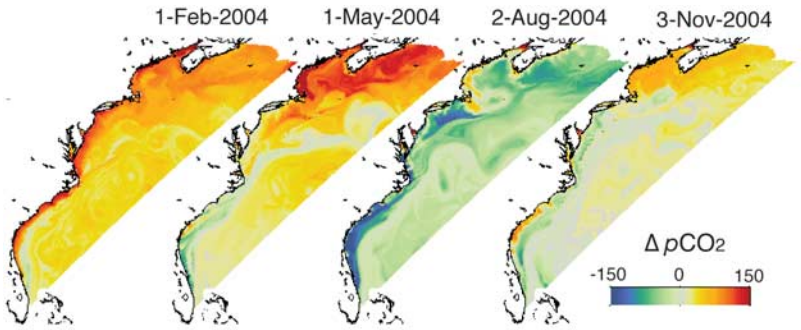

Figure 2. Snapshots of the simulated pCO_2 difference between the atmosphere and surface ocean for the baseline simulation. Positive values indicate uptake of atmospheric CO_2 by the ocean.

Table 1. Model-Derived Estimates of Carbon Fluxes for 2004 and 2005 for Five Combinations of Sub-regions Defined in Figure 1[a]

	Area (10^{10} m^2)	Total Air-Sea CO_2 Flux (10^{10} mol C yr^{-1})		Area Normalized Air-Sea CO_2 Flux (mol C m^{-2} yr^{-1})		Biologically Driven Fraction of CO_2 Flux (%)		Horizontal Divergence of Organic Carbon (10^{10} mol C yr^{-1})	
		2004	2005	2004	2005	2004	2005	2004	2005
MAB	8.62	8.98	6.29	1.04	0.73	92	58	4.25	2.97
NS&GB + GOM	16.74	32.8	23.1	1.96	1.38	52	30	8.89	9.52
SS	12.09	28.4	27.4	2.35	2.26	56	23	4.25	5.21
MAB SB + SW	20.35	20.8	15.8	1.02	0.78	11	3	—	—
SS SB + SW	25.10	44.4	36.8	1.77	1.47	27	5	—	—

[a]Positive air-sea fluxes are into the ocean. The biologically driven fraction of the air-sea flux was calculated by differencing the baseline and the no-bio simulations (as described in section 2). All other fluxes are for the baseline simulation.

coastal regions mostly driven by increases in solubility due to cooling. In May, DIC is strongly undersaturated in the Gulf of Maine and on the Scotian Shelf due to carbon uptake during the spring bloom, resulting in large uptake of atmospheric CO_2. In August, CO_2 is released in most of the domain as solubility decreases during warming and due to respiration of organic matter. Again the largest fluxes occur on the shelf. In November, the CO_2 flux has switched back to uptake in the Gulf of Maine (GOM) and on the Scotian Shelf (SS) where winter cooling has begun, but not yet on Georges Bank (GB) and in the MAB.

[9] We integrated the modeled air-sea flux of CO_2 and the horizontal divergence of organic carbon spatially for the regions shown in Figure 1 and in time for the years 2004 and 2005; we also calculated the fraction of the air-sea CO_2 flux driven by biological processes by difference with the no-bio model as described in section 2. These results are shown in Table 1. In both years the simulated uptake in the MAB is only about a third of the uptake in the NS&GB + GOM and SS regions. When comparing uptake normalized by area it appears that uptake increases with latitude with smallest fluxes in the MAB (1.04 and 0.73 mol C m^{-2} yr^{-1} for 2004 and 2005), larger fluxes in the NS&GB + GOM (1.96 and 1.38 mol C m^{-2} yr^{-1}) and highest fluxes on the SS ($\sim$2.3 mol C m^{-2} yr^{-1}). In both years the simulated uptake for the MAB agrees with the observational estimate of *DeGrandpre et al.* [2002] of 1.1 ± 0.69 mol C m^{-2} yr^{-1}.

[10] The simulated uptake in the stratified part of the MAB (9.0×10^{10} and 6.3×10^{10} mol C yr^{-1}) is roughly equal to the smaller, tidally mixed region that combines Nantucket Shoals and Georges Bank and has simulated annual uptakes of 9.7×10^{10} and 4.9×10^{10} mol C yr^{-1} for 2004 and 2005, respectively. This suggests that tidal mixing accelerates uptake on this shelf. The air-sea flux is generally smaller in 2005, which can be attributed to interannual variability. *Previdi et al.* [2009] assessed the magnitude of interannual variability that resulted from variations in atmospheric forcing for our model and found similar interannual variations in air-sea CO_2 fluxes.

[11] In the stratified MAB, the majority of carbon uptake is supported by biological processes ($\sim$90% and $\sim$60% in 2004 and 2005, respectively) compared to between one-fourth and one-half in the NS&GB + GOM and SS regions. The shelf regions are in strong contrast to the slope water regions MAB SB + SW and SS SB + SW, where only 3% and 27% of CO_2 uptake are supported by biological processes. The amount of organic carbon removed from the sub-regions by physical transport processes (i.e., the horizontal divergence of organic carbon) accounts for about half of the CO_2 uptake in the MAB, but smaller fractions—between approximately one-third and one-sixth—in the NS&GB + GOM and SS regions. It is roughly similar for the MAB and SS, but double for the NS&GB + GOM region. The organic carbon divergence is shown in spatially explicit form in Figure 3, which illustrates that organic carbon export is highly localized in a narrow strip along the shelf break, but greatly enhanced along the shelf break of Georges Bank, probably due to tidal mixing.

[12] The simulated uptake of atmospheric CO_2 in the slope water regions varies between 0.78 and 1.77 mol C m^{-2} yr^{-1} which is comparable to the values between 1 and 2 mol C m^{-2} yr^{-1} estimated by *Takahashi et al.* [2009] for this region. When comparing air-sea CO_2 fluxes between the shelf and adjacent slope water regions it appears that the simulated uptake normalized by area is similar between the MAB and MAB SB + SW regions. The simulated uptake for the SS SB + SW regions is similar to the uptake in the NS&GB + GOM, but smaller than on the SS. However, the mechanisms for carbon uptake between the shelves and adjacent slope regions are different with a much smaller contribution of biological processes in the slope regions.

4. Discussion and Conclusions

[13] We have presented model-based estimates of air-sea CO_2 flux, of the fraction of this flux that is driven by

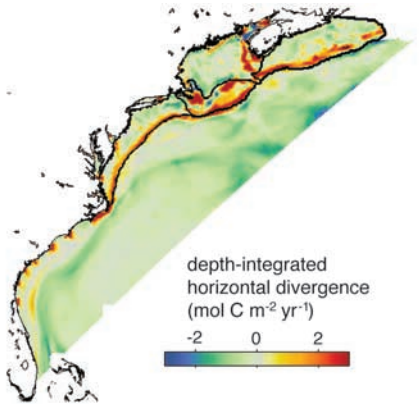

Figure 3. Spatial distribution of depth-integrated horizontal divergence of carbon (annual average for 2004) diagnosed from the baseline simulation. The boundaries of the sub-regions that we used for spatial integration (Table 1) are shown by the black lines.

biological processes, and of organic carbon transport for the eastern seaboard of North America. The latter two of these estimates would be very difficult to observe directly. Our estimates suggest that a latitudinal gradient exists with increasing area-normalized CO_2 uptake by the coastal ocean from the MAB, via Georges Bank and the Gulf of Maine to the Scotian Shelf. This gradient is coincident with a decrease in the relative contribution of biologically driven uptake. CO_2 uptake is enhanced over Georges Bank, as is the export of organic carbon (measured by its horizontal divergence), compared to the stratified shelf regions of the MAB and Scotian Shelf. It appears that tidal mixing, which is also responsible for the high levels of primary production observed on Georges Bank, enhances biologically driven carbon export in this region. This is in contrast to the North Sea where tidal mixing was observed to contribute to net-outgassing of CO_2 from the ocean [*Thomas et al.*, 2004].

[14] Our simulations suggest that the annual area-normalized uptake of atmospheric CO_2 in the shelf regions is not systematically larger than in the adjacent deep ocean regions. It appears that the horizontal export of water enriched in carbon is not large enough to drive a significant Continental Shelf Pump for the eastern margin of North America. While simulated uptake is larger on the shelf during winter and spring, simulated outgassing during the summer and fall is also larger on the shelf, leading to net annual fluxes roughly similar to those in the adjacent deep ocean regions. However, the mechanisms driving carbon export are qualitatively different between the shelf and the open ocean. On the shelf, vertical sinking of organic matter below the seasonal pycnocline is not sufficient for carbon export since subsequent winter mixing re-exposes this carbon at the surface; instead waters enriched in organic and inorganic carbon have to be transported horizontally across the shelf break. Export of organic matter off the shelf is simulated to occur only in a narrow band along the shelf break. Assuming that the horizontal divergence of organic carbon for the MAB (Table 1) equals export across the shelf edge, this would amount to $\sim 50 \times 10^6$ mol C yr^{-1} per km of along-shelf distance. The length of the shelf edge may be a more useful predictor of biological carbon export than the shelf area per se for coastlines that share the MAB characteristics of a broad, shallow continental shelf, bounded by a shelf-break density front. In addition to the region considered here, *Loder et al.* [1998] suggest other coasts in this category include West Florida, the northern Gulf of Mexico, South Brazil, and the South China Sea.

[15] **Acknowledgments.** We thank two anonymous reviewers for constructive comments. We gratefully acknowledge support from the NASA IDS U.S.Ecos project. KF was also supported by NSERC and CFI.

References

Bates, N. R. (2006), Air-sea CO_2 fluxes and the continental shelf pump of carbon in the Chukchi Sea adjacent to the Arctic Ocean, *J. Geophys. Res.*, *111*, C10013, doi:10.1029/2005JC003083.

Borges, A. V., B. Delille, and M. Frankignoulle (2005), Budgeting sinks and sources of CO_2 in the coastal ocean: Diversity of ecosystems counts, *Geophys. Res. Lett.*, *32*, L14601, doi:10.1029/2005GL023053.

Cai, W. J., M. Dai, and Y. Wang (2006), Air-sea exchange of carbon dioxide in ocean margins: A province-based synthesis, *Geophys. Res. Lett.*, *33*, L12603, doi:10.1029/2006GL026219.

Chassignet, E. P., H. E. Hurlburt, O. M. Smedstad, G. R. Halliwell, P. J. Hogan, A. J. Wallcraft, R. Baraille, and R. Bleck (2007), The HYCOM (HYbrid Coordinate Ocean Model) data assimilative system, *J. Mar. Syst.*, *65*, 60–83, doi:10.1016/j.jmarsys.2005.09.016.

DeGrandpre, M. D., G. J. Olbu, C. M. Beatty, and T. R. Hammar (2002), Air-sea CO_2 fluxes on the US Middle Atlantic Bight, *Deep Sea Res., Part II*, *49*, 4355–4367, doi:10.1016/S0967-0645(02)00122-4.

Dumont, E., J. Harrison, C. Kroeze, E. Bakker, and S. Seitzinger (2005), Global distribution and sources of dissolved inorganic nitrogen export to the coastal zone: Results from a spatially explicit, global model, *Global Biogeochem. Cycles*, *19*, GB4S02, doi:10.1029/2005GB002488.

Egbert, G. D., and S. Y. Erofeeva (2002), Efficient inverse modeling of barotropic ocean tides, *J. Atmos. Oceanic Technol.*, *19*, 183–204, doi:10.1175/1520-0426(2002)019<0183:EIMOBO>2.0.CO;2.

Fairall, C. W., E. F. Bradley, J. E. Hare, A. A. Grachev, and J. B. Edson (2003), Bulk parameterization of air-sea fluxes: Updates and verification for the COARE algorithm, *J. Clim.*, *16*, 571–591, doi:10.1175/1520-0442(2003)016<0571:BPOASF>2.0.CO;2.

Fennel, K., J. Wilkin, J. Levin, J. Moisan, J. O'Reilly, and D. Haidvogel (2006), Nitrogen cycling in the Middle Atlantic Bight: Results from a three-dimensional model and implications for the North Atlantic nitrogen budget, *Global Biogeochem. Cycles*, *20*, GB3007, doi:10.1029/2005GB002456.

Fennel, K., J. Wilkin, M. Previdi, and R. Najjar (2008), Denitrification effects on air-sea CO_2 flux in the coastal ocean: Simulations for the northwest North Atlantic, *Geophys. Res. Lett.*, *35*, L24608, doi:10.1029/2008GL036147.

Haidvogel, D. B., et al. (2008), Ocean forecasting in terrain-following coordinates: Formulation and skill assessment of the Regional Ocean Modeling System, *J. Comput. Phys.*, *227*, 3595–3624, doi:10.1016/j.jcp.2007.06.016.

Kalnay, E., M. Kanamitsu, R. Kistler, W. Collins, D. Deaven, L. Gandin, M. Iredell, S. Saha, G. White, and J. Woollen (1996), The NCEP/NCAR 40-year reanalysis project, *Bull. Am. Meteorol. Soc.*, *77*, 437–471, doi:10.1175/1520-0477(1996)077<0437:TNYRP>2.0.CO;2.

Lee, K., R. Wanninkhof, R. A. Feely, F. J. Millero, and T. H. Peng (2000), Global relationships of total inorganic carbon with temperature and nitrate in surface seawater, *Global Biogeochem. Cycles*, *14*, 979–994, doi:10.1029/1998GB001087.

Loder, J. W., W. C. Boicourt, and J. H. Simpson (1998), Western ocean boundary shelves, coastal segment (W), in *The Sea*, vol. 11, *The Global Coastal Ocean: Regional Studies and Syntheses*, edited by K. H. Brink and A. R. Robinson, chap. 1, pp. 3–27, John Wiley, New York.

Lozier, M. S., W. B. Owens, and R. G. Curry (1995), The climatology of the North Atlantic, *Prog. Oceanogr.*, *36*, 1–44, doi:10.1016/0079-6611(95)00013-5.

Millero, F. J., K. Lee, and M. Roche (1998), Distribution of alkalinity in the surface waters of the major oceans, *Mar. Chem.*, *60*, 111–130, doi:10.1016/S0304-4203(97)00084-4.

Previdi, M., K. Fennel, J. Wilkin, and D. Haidvogel (2009), Interannual variability in atmospheric CO_2 uptake on the northeast U.S. continental shelf, *J. Geophys. Res.*, doi:10.1029/2008JG000881, in press.

Sabine, C. L., R. A. Feely, N. Gruber, R. M. Key, K. Lee, J. L. Bullister, R. Wanninkhof, C. Wong, D. W. R. Wallace, and B. Tilbrook (2004), The oceanic sink for anthropogenic CO_2, *Science*, *305*, 367–371, doi:10.1126/science.1097403.

Takahashi, T., et al. (2009), Climatological mean and decadal change in surface ocean pCO_2, and net sea-air CO_2 flux over the global oceans, *Deep Sea Res., Part II*, *56*, 554–577, doi:10.1016/j.dsr2.2008.12.009.

Thomas, H., Y. Bozec, K. Elkalay, and H. J. W. deBaar (2004), Enhanced open ocean storage of CO_2 from shelf sea pumping, *Science*, *304*, 1005–1008, doi:10.1126/science.1095491.

Tsunogai, S., S. Watanabe, and T. Sato (1999), Is there a "continental shelf pump" for the absorption of atmospheric CO_2, *Tellus, Ser. B*, *51*, 701–712, doi:10.1034/j.1600-0889.1999.t01-2-00010.x.

Wanninkhof, R. (1992), Relationship between wind-speed and gas-exchange over the ocean, *J. Geophys. Res.*, *97*, 7373–7382, doi:10.1029/92JC00188.

Zeebe, R., and D. Wolf-Gladrow (2001), *CO_2 in Seawater: Equilibrium, Kinetics, Isotopes*, Elsevier, Amsterdam.

K. Fennel, Department of Oceanography, Dalhousie University, Halifax, NS B3H 4J1, Canada. (katja.fennel@dal.ca)

J. Wilkin, Institute of Marine and Coastal Sciences, Rutgers, State University of New Jersey, New Brunswick, NJ 08901-8521, USA.